

1-1-2004

Bandwidth dependence of the heterodyne efficiency in low coherence interferometry

C. Mujat

University of Central Florida

A. Dogariu

University of Central Florida

Find similar works at: <https://stars.library.ucf.edu/facultybib2000>

University of Central Florida Libraries <http://library.ucf.edu>

This Article is brought to you for free and open access by the Faculty Bibliography at STARS. It has been accepted for inclusion in Faculty Bibliography 2000s by an authorized administrator of STARS. For more information, please contact STARS@ucf.edu.

Recommended Citation

Mujat, C. and Dogariu, A., "Bandwidth dependence of the heterodyne efficiency in low coherence interferometry" (2004). *Faculty Bibliography 2000s*. 4593.

<https://stars.library.ucf.edu/facultybib2000/4593>

Bandwidth dependence of the heterodyne efficiency in low coherence interferometry

C. Mujat and A. Dogariu

School of Optics, University of Central Florida, P.O. Box 162700, Orlando, FL, USA
adogariu@mail.ucf.edu

Abstract: The effect of radiation bandwidth on the heterodyne detection process is discussed. We show that, although neglected in current formalisms, the spectral changes induced by the scattering process are decreasing the heterodyne detection efficiency. This effect depends on the bandwidth of the radiation used.

© 2004 Optical Society of America

OCIS codes: (290.0290) scattering, (040.2840) heterodyne, (170.4500) optical coherence tomography

References and links

1. D. Huang, E. Swanson, C.P. Lin, J.S. Schuman, W.G. Stinson, W. Chnag, M.R. Hee, T. Flotte, K. Gregory, C.A. Puliafito, and J.G. Fujimoto, "Optical coherence tomography," *Science* **254**, 1178-1181 (1991).
2. Y.T. Pan, R. Birngruber, J. Rosperich, and R. Engelhardt, "Low-coherence optical tomography in turbid tissue: theoretical analysis," *Appl. Opt.* **34**, 6564-6574 (1995).
3. J.M. Schmitt and A. Knüttel, "Model of optical coherence tomography of heterogeneous tissue," *J. Opt. Soc. Am. A* **14**, 1231-1242 (1997).
4. D. Levitz, L. Thrane, M.H. Frosz, P.A. Andersen, C.B. Andersen, J. Valanciunaite, J. Swartling, S. Andersson-Engels, and P.R. Hansen, "Determination of the optical scattering properties of highly scattering media in optical coherence tomography images," *Opt. Express* **12**, 249-259 (2004), <http://www.opticsexpress.org/abstract.cfm?URI=OPEX-12-2-249>.
5. W. Drexler, U. Morgner, F.X. Kärtner, C. Pitris, S.A. Boppart, X.D. Li, E.P. Ippen, and J.G. Fujimoto, "In vivo ultrahigh-resolution optical coherence tomography," *Opt. Lett.* **24**, 1221-1223 (1999).
6. G. R. Osche, "Optical detection theory for laser applications," Wiley Series in Pure and Applied Optics, 2002.
7. E. Wolf and D.F.V. James, "Correlation induced spectral changes," *Rep. Prog. Phys.* **59**, 771-812 (1996).
8. A. Dogariu and E. Wolf, "Spectral changes produced by static scattering on a system of particles," *Opt. Lett.* **23**, 1340-1342 (1998).
9. J.M. Schmitt and G. Kumar, "Optical scattering properties of soft tissue: a discrete particle model," *Appl. Opt.* **37**, 2788-2797 (1998).
10. A. Dogariu, "Volume scattering in random media," in *Handbook of Optics*, vol III, M. Bass, J.M Enoch, E.W. van Stryland and W. Wolfe, eds. (McGraw-Hill, New York, NY, 2001), pp. 3.1-3.18.

Low-coherence interferometry, also known as optical coherence tomography (OCT) [1] is an optical technique that has been greatly developed over the last years, in response to the increasing interest in noninvasive techniques for in-vivo tissue imaging and characterization. Based on the different scattering properties of tissue constituents, this technique acquires a backscattering map of the tissue sample which is inherently related to the tissue morphology and physiology. However, extracting such quantitative information from an image is not straightforward, especially for highly scattering tissues. Not only the multiple scattering and interference effects

decrease the image contrast but, as we will see in the following, the detection process is also influencing the outcome. In an attempt to improve the depth resolution of this interferometric technique, the bandwidth of the incident radiation has been increased considerably. In spite of this trend, all of the models introduced to explain OCT images of heterogenous tissue, use a quasimonochromatic description of the heterodyne detection process [2, 3, 4]. Although this might not be a problem when the bandwidth is small compared to the central wavelength (for example $\Delta\lambda = 30nm$ centered at $\lambda_0 = 800nm$), one must cautiously describe the process for larger bandwidths.

In this work we address the problems that arise in OCT due to different spectral composition of the reference and the sample beams. Dispersion, absorption, and scattering processes in the tissue are all sources of differences between the spectral compositions of the reference and sample beams. They are generally system specific and, at least for the scattering process, their effect is not obvious. Let us take for instance the process of building an OCT *en-face* image which requires scanning the sample beam across the tissue. In this case, the contrast between different regions is given by the specific scattering properties (reflectance) of each region. However, such regions are usually highly structured and spatially inhomogeneous and they could lead to different spectral compositions of the scattered beam. In other words, the contrast between different regions will be system specific. To compensate for dispersion effects in optical fibers and refractive optics more or less elaborated schemes have been developed and integrated in OCT systems [5]. On the other hand, accounting for dispersion, absorption and scattering induced effects in the sample implies a priori knowledge of the properties of the investigated tissue.

For the purpose of this study we will limit the discussion to scattering induced-changes in the heterodyne detection efficiency. Following the heterodyne efficiency definition given by Osche [6], and assuming that the responsivity of the detector is uniform across the wavelength range of interest we consider the heterodyne efficiency of a polychromatic interferometric system to be

$$\eta = \frac{\left| \int \sqrt{S_0(\omega)S(\omega)} d\omega \right|^2}{\int S_0(\omega) d\omega \int S(\omega) d\omega}, \quad (1)$$

where $S_0(\omega)$ and $S(\omega)$ are the spectral densities of the reference and sample beam, respectively. Of course, in general, $\eta \leq 1$ and the equality holds only when the sample beam is not spectrally modified, i.e. when $S(\omega) = \alpha S_0(\omega)$. For most practical situations however $S(\omega) = M(\omega)S_0(\omega)$, and $\eta < 1$. The spectral modifier $M(\omega)$ describes the spectral changes in the sample beam and although the instrument dependent dispersion effects can also be included in $M(\omega)$, they are not considered here because they can be easily accounted for by instrument calibration. We thus consider that $M(\omega)$ describes only the scattering induced changes. In analogy with the mixing theorem, that states that for any mismatch in phase and amplitude between the local oscillator and the signal beam, the detected signal will be less than optimal, the above definition in Eq.(1) implies that any mismatch between the spectral density of the reference and sample beams will decrease the signal detected in the heterodyne process.

Not long ago, a number of situations have been described where correlated scattering induces spectral changes [7]. To obtain the wavelength dependent spectral modifier for situations pertinent to tissue constituents we will follow the procedure outlined by Dogariu and Wolf [8], that describes the spectrum of the light scattered by a static system of particles at a distance r to be given by

$$S(r\mathbf{u}, \omega) = \frac{1}{r^2} \left\langle \left| \tilde{F}(k(\mathbf{u} - \mathbf{u}_0), \omega) \right|^2 \right\rangle S_0(\omega), \quad (2)$$

where $\tilde{F}(k(\mathbf{u}-\mathbf{u}_0), \omega)$ is the three dimensional Fourier transform of the scattering potential, and \mathbf{u} and \mathbf{u}_0 are the scattering and the illumination directions, respectively. As the OCT systems acquire a backscattering map of the tissue, we only deal in this study with $\mathbf{u} = \mathbf{u}_0$, no other angularly dependent chromatic effects are considered.

To illustrate the influence of the scattering-induced spectral changes on the heterodyne detection efficiency, let us consider systems of identical, spherical particles, illuminated with an incident field whose spectrum is Gaussian, centered at $\lambda = 800nm$ and has a variable bandwidth ($\Delta\lambda = 50 - 150nm$). As OCT is mainly used for tissue characterization, the properties of the scattering media were chosen to be close to those of typical tissue [9], with average refractive index contrast 1.05 (1.42 - scattering centers; 1.354 - background medium), and sizes from $50nm$ to $25.6\mu m$ (organelles - hundreds of nm size; cell nuclei - μm size). As the concentration of the scattering centers in biological tissue is sometimes very high, correlated scattering was taken into account, in this case by means of the Percus-Yevick approximation for the structure function $Y(u)$. A measure of the degree of correlation between the fields scattered by individual scattering centers, the structure function is dependent on the relative positions of the scattering centers [10]

$$Y(\mathbf{u}) = \frac{1}{N} \sum_{i,j=1}^N \exp(-i\mathbf{u} \cdot (\mathbf{r}_i - \mathbf{r}_j)) \quad (3)$$

where \mathbf{r}_i denotes the position of the i scattering center. After ensemble averaging over the scattering volume V , the structure factor can be calculated as

$$Y(\mathbf{u}) = 1 + \langle \exp(-i\mathbf{u} \cdot (\mathbf{r}_i - \mathbf{r}_j)) \rangle = 1 + \rho \int G(\mathbf{r}) \exp(-i\mathbf{u} \cdot \mathbf{r}) d\mathbf{r} \quad (4)$$

where $G(\mathbf{r})$ is the pair correlation function, that describes the statistical properties of the spatial arrangement of the scattering centers, and ρ is the scattering centres concentration. In a Percus-Yevick approximation for the structure function, the three dimensional Fourier transform of the scattering potential is

$$\left| \tilde{F}(k(\mathbf{u}-\mathbf{u}_0), \omega) \right|^2 = |f_1(\mathbf{u}, \mathbf{u}_0; \omega)|^2 = \frac{\sigma_t}{4\pi} p_{PY}(\mathbf{u}, \mathbf{u}_0; \omega) \quad (5)$$

where $f_1(\mathbf{u}, \mathbf{u}_0; \omega)$ is the scattering amplitude (generally complex) of the scattering center in the direction \mathbf{u} when illuminated from \mathbf{u}_0 , and $p_{PY}(\mathbf{u}, \mathbf{u}_0; \omega)$ is the Percus-Yevick modified phase function defined as the product between the single scattering phase function and the structure factor $Y(\mathbf{u})$ of the scattering system

$$p_{PY}(\mathbf{u}, \mathbf{u}_0; \omega) = p(\mathbf{u}, \mathbf{u}_0; \omega) Y(\mathbf{u}). \quad (6)$$

The scattering-induced spectral changes, calculated in these conditions for various volume fractions of $200nm$ radius scatterers are presented in Fig.1. It is clearly seen that the spectrum of the incoming radiation $S_0(\omega)$ is dramatically modified due to scattering; it changes from a Gaussian shape to a two-lobed distribution. Moreover, note that the collective scattering effects influence the shape of the scattered spectrum as well. As can be seen, the spectral density for 5% volume fraction is quite different than the one corresponding to 45% volume fraction.

As a consequence of the concentration dependent spectra of the scattered light, the heterodyne detection efficiency changes also with the concentration as shown in Fig. 2. Note that the efficiency η decreases with more than 10% as the spectral width of the incoming radiation increases, indicating that precautions must be taken when increasing the spectral width of the source. Calculating the efficiency η as a function of the volume fraction $f(\%)$ for different scattering systems, we have also determined that this variation is influenced by the size of the scattering centers and the refractive index contrast.

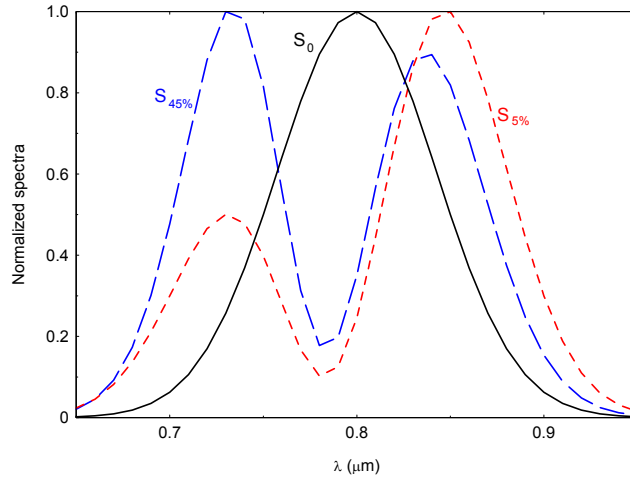


Fig. 1. Spectrum of the scattered light for monodisperse systems of scatterers with radius of $200nm$ and two different volume fractions of 5% and 45% as indicated. For comparison, the spectrum of the incident light S_0 is also included ($\Delta\lambda = 100nm$).

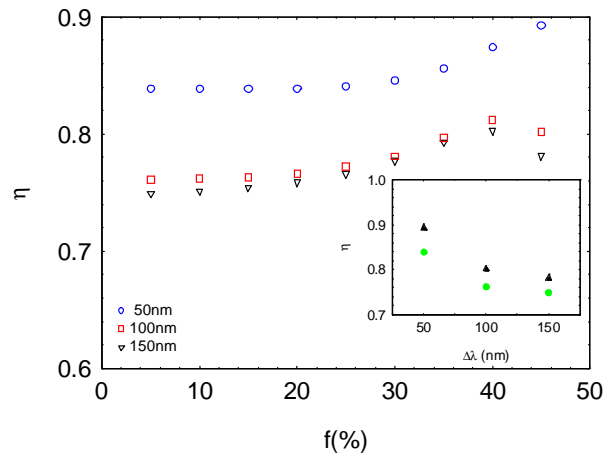


Fig. 2. Heterodyne detection efficiency evaluated from Eq.(1) as a function of the volume fraction of the scattering centers ($200nm$ radius; 1.05 refractive index contrast). The three curves represent the detection efficiency for different spectral widths $\Delta\lambda$ of the incident beam as indicated. The inset presents the heterodyne detection efficiency versus the spectral width of the incident radiation, for two different concentrations of scatterers 45% (triangles) and 5% (circles).

To illustrate the effects of the scattering-induced spectral changes on the contrast detected between regions with different scattering properties we considered two different OCT imaging scenarios: (a) a system of identical scatterers with the volume fraction varying across the detected plane and (b) different systems of scatterers. As an OCT image is built by scanning the sample beam onto the tissue, transversally, pixel by pixel, this contrast is a measure of the image quality. Not only the contrast needs to be high in order to discern between different tissue constituents, but its value should also be representative of the difference in the scattering

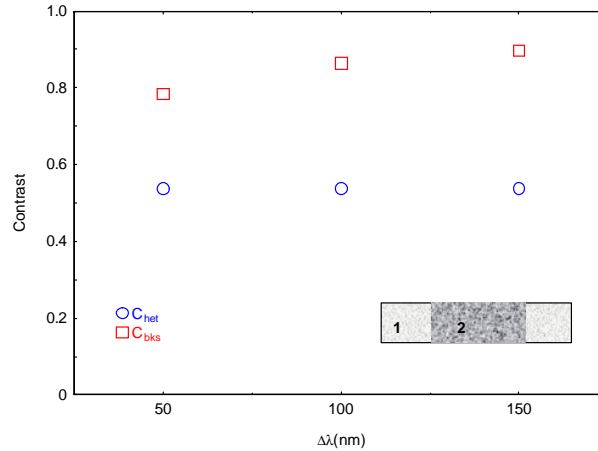


Fig. 3. Image contrasts C_{het} and C_{bks} versus the bandwidth of the incident radiation. Regions 1 and 2, as indicated in the inset, have scattering centers of the same size $2.5\mu m$ but different volume fractions: 5% and 45%, respectively. The relative refractive index between the scattering centers and the background is $n_s/n_b = 1.05$.

properties when a quantitative analysis is desired. In a direct backscattering measurement, the optical contrast between two regions with different scattering properties is determined by evaluating the differences in the backscattering cross-section per unit area of the region (considered to be a slab of thickness equal to the coherence length l_c of the incident radiation)

$$C_{bks} = \left| \frac{R_{b1} - R_{b2}}{R_{b1} + R_{b2}} \right|, \quad (7)$$

where

$$R_b = \frac{\sigma_b}{2\sigma_t} [1 - \exp(-2\rho\sigma_t l_c)] \quad (8)$$

and σ_b and σ_t are the backscattering and the extinction cross sections, respectively. The scattering cross-sections are integrated over the entire wavelength range and the density of scatterers is denoted by ρ . Similar to Eq. (7), the contrast for the heterodyne detection process can be calculated as

$$C_{het} = \left| \frac{R_{het1} - R_{het2}}{R_{het1} + R_{het2}} \right| \quad (9)$$

where R_{het} represents the heterodyne signal detected with the corresponding efficiency as defined in Eq. (1).

The image contrasts obtained by either heterodyne detection C_{het} or by a direct backscattering measurement C_{bks} , are presented in Fig. 3 and Fig. 4 for the two sensing scenarios described above. The sizes and refractive index contrast used have been chosen to be representative for tissue constituents (organelles - hundreds of nm size; cell nuclei - μm size). The scattering coefficients for these systems are $\mu_s = 5 - 40 mm^{-1}$ for $200 nm$ size of the scattering centers, and $\mu_s = 40 - 400 mm^{-1}$ for $2.5\mu m$ size of the scattering centers, values similar to those measured in human tissue [9, 4].

As shown in Fig. 3 and Fig. 4, the contrast determined by the heterodyne detection between regions with different optical properties is quite different in magnitude from the one obtained in

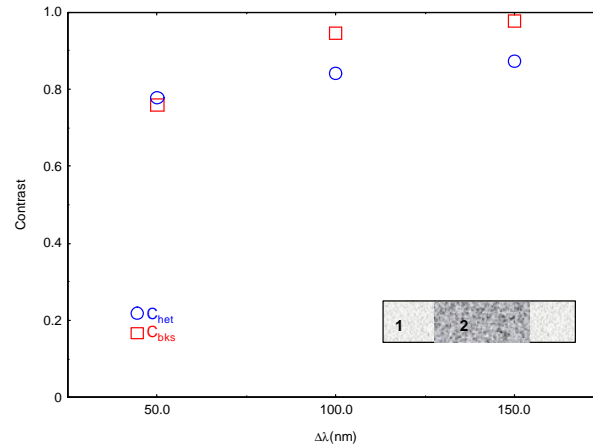


Fig. 4. Image contrasts C_{het} and C_{bks} versus the bandwidth of the incident radiation. Regions 1 and 2 have same volume fractions of the scattering centers (5%) but different sizes: $0.2\mu m$ and $2.5\mu m$, respectively. The relative refractive index between the scattering centers and the background is $n_s/n_b = 1.05$.

a direct backscattering measurement. Moreover, one can see that the contrast variation with the bandwidth is different for the two methods of detection, hence this effect needs to be carefully accounted for in a quantitative assessment of the heterodyne image.

The present treatment did not include any depth degradation effects due to the multiple scattering processes and loss of spatial coherence of the sample beam, as described by Levitz *et al.* [4]. However, these effects could be included in a generalization of this formalism in the space frequency domain.

Our results demonstrate that, although neglected in current formalisms, the spectral changes induced by scattering alone will in general decrease the detection efficiency in a heterodyne detection process. The effect is stronger when the bandwidth of the incoming radiation is increased and it is dependent on the specific scattering system. The bandwidth dependence needs to be carefully considered when OCT techniques are to be used as a quantitative tool for characterizing inhomogeneous media.

Acknowledgments

We thank Mohamed Salem for helpful discussions related to this work.